CONCRETE LIBRARY OF JSCE NO. 37, JUNE 2001

EVALUATION OF PULLOUT OF LONGITUDINAL BARS FROM FOOTINGS OF RC PIERS UNDER CYCLIC LOADING WITH LARGE DYNAMIC RANGE

(Translation from Proceedings of JSCE, No.648/V-47, May 2000)


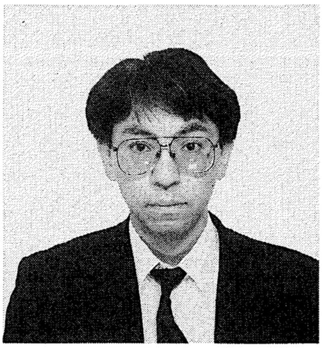
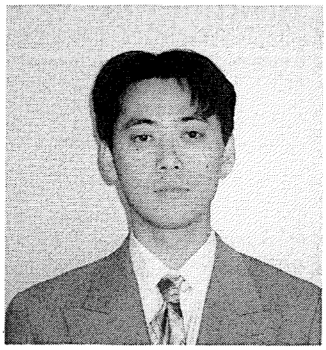

Tadayoshi ISHIBASHI Kaoru KOBAYASHI Takuya UMIHARA

This paper proposes a method for evaluating the amount of pullout of longitudinal bars from the footings of RC bridge piers and RC columns subject to cyclic loading with a large dynamic range. The evaluation of deformation capacity during earthquakes is based on this pullout of steel bars from the footings. A study is also made on a method of obtaining the pullout of steel bars from the footings of reinforced concrete bridge piers and RC columns where the deformation capacity is a ductility ratio of more than 10, resulting in a method capable of accurate results.

Keyword : *Pullout, Bond-Slip-Strain Relationship, Cyclic Loading Test*

Tadayoshi Ishibashi is a manager at the Construction Division of East Japan Railway Company, Tokyo, Japan. He obtained his Doctor of Engineering degree from the University of Tokyo in 1984. His research interests include the seismic design of concrete structures for railways.

Kaoru kobayashi is assistant director of the Construction Division of East Japan Railway Company, Tokyo, Japan. His research interests include the seismic design of concrete structures for railways . He is a member of the JSCE.

Takuya Umihara is the member of the Construction Division of the Engineering Department at Hokkaido Railway Company. His research relates to the development of methods of seismic retrofitting of reinforced concrete structures. He is a member of the JSCE.

1. INTRODUCTION

When earthquake forces act on a structure such as a reinforced concrete pier or column, the resulting reversed cyclic loading causes deformation behavior consisting of lateral bending and shear displacement of the main structure, as well as other lateral displacements evident as pullout of longitudinal reinforcing bars from the footings. It has been reported[1] that the lateral displacement contributed by pullout of longitudinal reinforcing bars accounts for much of the total lateral displacement. In order to properly evaluate the ductile capacity of RC piers or RC columns, it is necessary to establish a method of calculating the lateral displacement resulting from this pullout.

The Hyogoken-Nanbu Earthquake of 1995 damaged many structures. As a result of this event, Seismic Performance of RC structures is demanded deformation ability [2]. Where the deformation range is large, meaning a ductility ratio of around 10, there are few examples of research in which pullout of the longitudinal reinforcing bars from footings is calculated, and in those that do exist, many issues require further clarification.

This research focuses on the amount of reinforcing bar pullout from footings as a basis for the deformation performance evaluation of RC piers or RC columns. The aim is to propose an equation for reinforcing bar pullout that can be applied to cyclic loading with a large deformation range (corresponding to a ductility ratio of around 10).

In this study, the amount of reinforcing bar pullout under cyclic loading is measured directly in one RC column specimen. This specimen contained hoop reinforcing bars in a comparatively dense arrangement designed to result in a member ductility of around 10. Space was vacated on the side of footings, and displacement meters were installed to measure the amount of reinforcing bar pullout from footings. These displacement meters were fastened to reinforcing bars via wires over the surface of the footings, and the pullout of the reinforcing bars in cyclic loading was measured directly.

Stable displacement was observed until the ultimate displacement, which is defined as the deformation capacity of the member. It was confirmed that experimental results agreed well with analytical results, when Shima's model for bond-slip-strain relationship [3] (it is expressed as "τ-s-ε" in this paper) and bond deterioration zone are considered in analysis.

From the analytical results, Sin's model[4] of reinforcing bar strain-slip under monotonic loading is modified into a proposed equation for the amount of reinforcing bar pullout from footings under large cyclic deformation (equivalent to a member ductility ratio of around 10).

2. Experimental outline

2.1 Specimen shape and properties

An outline of the specimen and a drawing of its bar arrangement are shown in Figure 1 and Figure 2, respectively. The properties of the specimen are given in Table 1. These properties such as the quantity of lateral reinforcing bars and the ratio of shear strength to flexural strength (Vy*a/Mu, where Vy: shear strength; Mu: flexural strength; a: shear span).were determined in reference to previous studies[5] about ductile capacity of RC members

The embedded length of longitudinal bars is over 30D in the footings. Further, the ends of longitudinal bars in the footings were made into right-angle hook with more than 20D length, in order to avoid the slip at the ends of re-bars. With regard to specimen K1, the pullout of an anchored bar from the footings is measured directly to satisfy recent interest in the pullout of anchored reinforcing bars under cyclic loading.

2.2 Measurement outline

During cyclic loading tests on the specimens, longitudinal and lateral reinforcing bar strains were measured with wire-strain-gauges, and lateral displacements above the footings were measured with lateral displacement meters. In the case of specimen K1, the pullout of an anchored bar from the footings was directly measured along with the items mentioned above.

Table 1 Properties of specimens

specimen	specimen propaties					longitudinal reinforcing bar					lateral reinforcing bar		average axis stress σ (N/mm²)	cyclic loading pattarn	experiment value					calculation value			comparison		
	b (mm)	h (mm)	effective height d (mm)	shear span a (mm)	a/d	diameter of bar	number	reinforcing bar ratio (%)	number of tensil bar	Reinforcing bars classification	lateral reinforcing bars arrangement	reinforcing bar ratio (%)			yield displacement δy(mm)	ultimate displacement δu(mm)	ductility ratio μ =δu/δy	yield load Py (kN)	maximum load Pmax (kN)	yield load Pyc (kN)	maximum load Pmaxc (kN)	lateral load that cover concrete was removed and calculated Puyc (kN)	Py/Pyc	Pmax/Pmaxc	Py/Puyc
No1	400	400	360	1150	3.19	D19	16	2.865	5	T3	D13-1@125	0.507	0.98	A	6.50	48.88	7.52	213.7	300.6	203.9	255.8	231.5	1.05	1.17	0.92
No2	400	400	360	1150	3.19	D19	16	2.865	5	T3	D13-1@70	0.905	0.98	A	7.56	70.93	9.38	222.3	298.6	201.3	251.4	228.3	1.10	1.19	0.97
No3	400	400	360	1150	3.19	D19	16	2.865	5	T3	D13-1@40	1.584	0.98	A	7.14	66.73	9.35	223.2	305.0	206.6	259.8	234.5	1.08	1.17	0.95
No4	400	400	360	1150	3.19	D16	16	1.986	5	T2	D13-1@90	0.704	0.49	A	6.35	58.36	9.19	179.9	232.3	149.3	188.8	170.8	1.21	1.23	1.05
No5	400	400	360	1150	3.19	D16	16	1.986	5	T2	D13-1@50	1.267	1.96	A	6.15	61.29	9.96	193.2	263.3	177.9	218.7	193.5	1.09	1.20	1.00
No6	400	600	550	1150	2.09	D13	12	0.634	4	T1	D13-1@90	0.704	0.98	A	6.72	48.05	7.15	181.1	237.3	149.5	181.5	162.8	1.21	1.31	1.11
No7	400	350	300	1250	4.17	D22	16	4.424	5	T4	D13-1@90	0.704	0.98	A	9.95	89.30	8.97	222.6	310.5	216.9	264.3	215.0	1.03	1.17	1.04
No8	350	350	310	1150	3.71	D19	16	3.742	5	T3	D16-1@50	2.270	4.90	A	9.15	87.31	9.54	202.2	275.3	210.4	244.6	212.7	0.96	1.13	0.95
a1	400	400	360	1150	3.19	D19	16	2.865	5	T7	D13-1@80	0.792	0.98	B	8.13	73.41	9.03	218.9	282.9	203.3	254.8	230.7	1.08	1.11	0.95
a2	400	400	360	1150	3.19	D19	16	2.865	5	T7	D13-1@60	1.056	0.98	B	7.66	82.05	10.71	214.6	278.3	201.2	251.1	228.2	1.07	1.11	0.94
a3	400	400	360	1150	3.19	D16	16	1.986	5	T6	D13-1@70	0.905	0.49	B	6.18	76.78	12.43	143.5	203.9	148.6	187.6	169.9	0.97	1.09	0.84
a4	400	400	360	1150	3.19	D13	16	1.267	5	T5	D13-1@80	0.792	0.98	B	8.31*	41.17	4.95*	109.3	148.4	102.9	127.9	114.2	1.06	1.16	0.96
a5	400	400	360	1150	3.19	D13	16	1.267	5	T5	D13-1@140	0.453	0.98	B	5.41	47.89	8.85	114.1	145.3	103.0	128.9	114.6	1.11	1.13	1.00
a6	400	400	360	1150	3.19	D19	16	2.865	5	T7	D13-1@50	1.267	0.98	B	6.92	90.17	13.02	222.4	307.3	206.1	259.0	233.9	1.08	1.19	0.95
a7	400	400	360	1150	3.19	D19	16	2.865	5	T7	D13-1@60	1.056	0.98	A	6.57	71.49	10.89	209.6	309.2	205.9	258.8	233.7	1.02	1.19	0.90
a8	400	400	360	1150	3.19	D16	16	1.986	5	T6	D13-1@120	0.528	0.98	B	6.54	61.27	9.36	175.1	222.9	155.6	193.4	174.4	1.13	1.15	1.00
a9	400	400	360	1150	3.19	D19	16	2.865	5	T7	D16-1@60	1.655	0.98	B	6.80	90.66	13.33	208.0	292.3	200.0	248.8	226.9	1.04	1.17	0.92
a10	400	700	660	1000	1.52	D19	16	1.842	5	T7	D13-1@60	1.056	0.98	B	4.60	49.34	10.73	444.8	640.8	434.6	643.2	605.2	1.02	1.00	0.74
a11	500	500	460	1150	2.50	D19	16	1.834	5	T7	D13-1@60	0.845	0.98	B	5.80	71.62	12.35	265.8	366.4	281.0	355.8	324.3	0.95	1.03	0.82
K1	400	400	360	1150	3.19	D19	16	2.865	5	T8	D13-1@60	1.056	0.98	B	5.8	78.10	13.47	208.7	274.4	196.7	243.7	223.3	1.06	1.13	0.93

*: lateral displacement became big because it had already had loaded around Pmax at the time of 1δy.

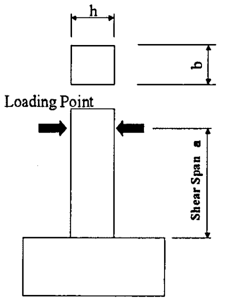

Figure 1 Outline of Specimens

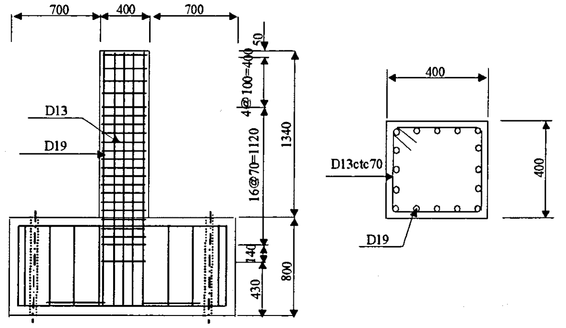

Figure 2 Arrangement of Reinforcing Bars (Specimen 2)

Measurements were carried out as follows. Displacement meters were installed in box-shaped cutouts prepared in advance, and the wires connecting meters to longitudinal reinforcing bars passed over the footing surface. These wires were protected with stainless steel piping of diameter 10 mm; a silicone tube within the pipe ensured that there was no need to consider friction between the pipe wall and the wire. To check the direct measurement method for pullout of anchored bars, another kind of measurement was provided. A steel bar of Φ6mm penetrates the specimen at a height of 5cm above the surface of footing, and distance between the steel bar and the footing was measured. In the event of the cover concrete spalling or the uncovering of longitudinal reinforcing bars, the first measurement method of pullout becomes less reliable and the measured values are reliable until the load starts decreasing (before post-peak range). A sketch of the method used to measure pullout of anchored bar from the footing is given in Figure 3. Photograph 1 shows a displacement meter installed in a footing cutout.

2.3 Outline of Cyclic Loading Test

Cyclic loading was carried out as shown in Figure 4. For the tests, the footing of the specimen was fixed to the floor with PC steel bars. An axial load was then introduced using a vertical jack (average axis compression stress: σ=0.49-4.90 N/mm2), and cyclic loading was applied to the top of the specimen statically as the load point. Cyclic loading was increased to the yield displacement (δy) under load control. Then, for lateral displacements greater than δy, the lateral displacement by the integer of δy by displacement control was given.

In Table 1, cyclic loading pattern A consists of one cycle each for even numbers 2δy, 4δy, etc. After a cyclic loading step in which a lateral load decline occurs, cyclic loading is loaded 1δy each increased lateral displacement and three cycles. After 2δy rest, A pattern B had loaded to each of every 1δy and one cycle.

Two cyclic loading patterns were used. Cyclic loading pattern A was implemented first. However, in cyclic loading tests targeting large deformations of about 10 or more, as in these tests, the longitudinal reinforcing

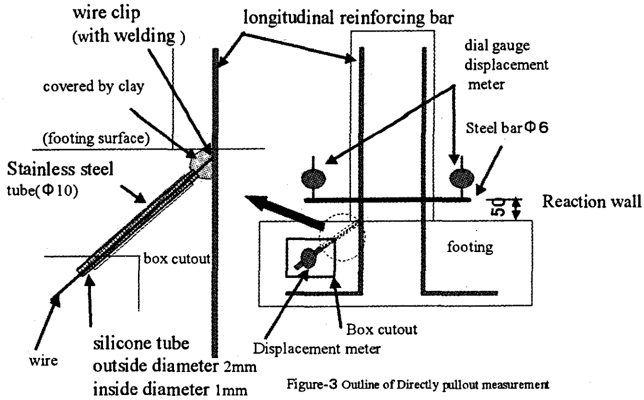

Figure 3 Reinforcing Bar Pullout Measurements

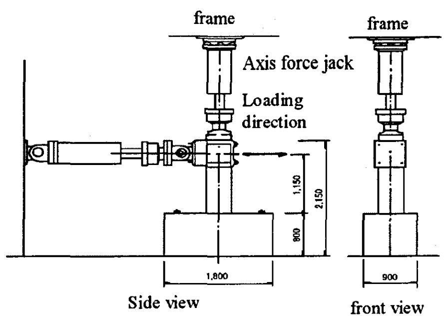

Figure 4 Test Setup

bars sometimes rupture due to low cycle fatigue. Pattern B was used for some specimens as shown in Table 1 because such failures have never been confirmed in past earthquakes and because reinforcing bar rupture makes no sense in the context of these experiments.

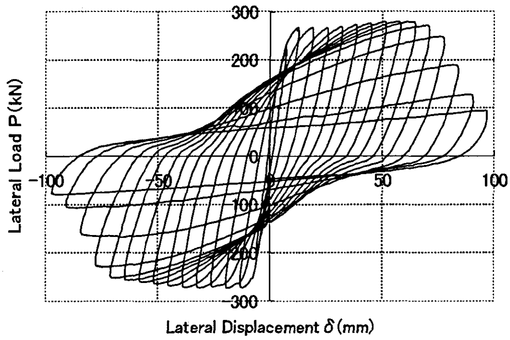

Figure 5 Lateral Load-Lateral Displacement Relationship (Specimen K1)

3. Results Of Experiments

3.1 Yielding Load / Maximum Load

The experimental values of yield load (Py) and maximum load (Pmax) are shown in Table 1.The experimental yield load is the lateral load at the point when the lateral displacement of the specimen reaches the yield displacement at the horizontal loading position.

As for the maximum load, ultimate concrete strain was calculated as 0.0035 from the Railroad Structure Design Standard (Concrete Structure Volume)[6]. The material strength used for these calculations was the actual strength of the material used in the experiments, as shown in Table 2.

3.2 Load–Displacement Relationship

An example of a load-displacement curve obtained from a cyclic loading test is shown in Figure 5. The ductile capacity of each specimen was evaluated as the value of ductility when δu was divided by δy. Here, δy is the yield displacement of each specimen. The ultimate displacement, δu, of each specimen is the maximum lateral displacement and is lower than the yield load of the specimen.

Table 2 Concrete and Steel Characteristics

specimen	concrete strength(N/mm^2)		longitudinal reinforcing bar		
	column	footing	yield stress fsyk (N/mm^2)	yield strain εy	young's modulus Es (N/mm^2)
N1	27.4	28.0	378.3	2068	182921
N2	23.5	28.2	378.3	2068	182921
N3	31.9	27.1	378.3	2068	182921
N4	28.2	24.3	397.2	2153	184484
N5	33.6	24.9	397.2	2153	184484
N6	32.3	27.8	359.1	1986	180802
N7	33.7	26.9	379.1	2163	175249
N8	32.4	31.3	378.3	2068	182921
A1	26.4	31.4	378.4	2069	182880
A2	23.3	29.0	378.4	2069	182880
A3	26.8	24.8	397.2	2156	184227
A4	28.4	27.5	358.3	1980	180954
A5	29.1	29.4	358.3	1980	180954
A6	30.9	28.6	378.4	2069	182880
A7	30.7	30.3	378.4	2069	182880
A8	23.8	30.0	397.2	2156	184227
A9	21.7	22.1	378.4	2069	182880
A10	22.3	21.8	378.4	2069	182880
A11	24.6	24.4	378.4	2069	182880
K1	19.4	19.6	375.1	2061	182020

4. Examination of longitudinal reinforcing bar pullout

4.1 Outline of examination method using τ-s-ε relationship

The amount of pullout of longitudinal reinforcing bar (S) from the footings can be calculated from Equation

(1). The embedded length of reinforcing bars is adequate and they have a right-angle hook at the tip, so slip is clearly not a problem. Therefore, the amount of pullout is the actual integrated value of strain ε at each point on the reinforcing bar from the tip to the surface of the footings.

$$S = \int \varepsilon \, dx \qquad (1)$$

Within the footings, the strain of the longitudinal reinforcing bars decreases. This is because there is a bonding force between the reinforcing bars and the concrete.
In section Δx, the decrease in stress Δσ is calculated using Equation (2):

$$\Delta \sigma = \pi \cdot \phi \cdot \Delta x \cdot \tau / As \qquad (2)$$

Where,
Δx: section
Φ: reinforcing bar diameter
τ: bond stress between the reinforcing bars and concrete
As: sectional area of reinforcing bars

Consequently, the amount of pullout of longitudinal reinforcing bars can be analyzed using the following process. First, the pullout of a longitudinal reinforcing bar is estimated on the surface of the footing. The following value, is calculated in the inside from the surface of footing. Values to be calculated are the bond force, the reduction in reinforcing bar stress, and the reinforcing bar strain. First, the integrated reinforcing bar strain is subtracted from the estimated pullout of longitudinal reinforcing bars. The calculation is iterated until the amount of pullout at the tip of the reinforcing bars is approximately zero. It can get the quantity of pullout of the reinforcing bars by changing the supposition of the quantity of pullout of the surface of footing and repeating it and calculating it in the analysis. The analytical procedure is shown in Figure 6. It is necessary to obtain the relationship between the bond stress between the reinforcing bars and the concrete and the reinforcing bar slip. Shima et al. proposed Equation (3) on the basis of axial tension experiments on embedded reinforcing bars in mass concrete. This equation indicates the relationship between bond stress (τ) and slip (s) and strain (ε).Further, Shima's experiment was carried out in the range where there is no bonding at the loaded end. As a result, bonding at the load end is prevented from influencing the experiment results. After the reinforcing bars yield, Equation (3) can be applied.[7]

$$\tau / f'ck = 0.73(\ln(1+5s))^3/(1+\varepsilon \times 10^5) \qquad (3)$$

Where,
s: normalized slip=1000*S/D
τ: bond stress
f'ck : concrete strength,
S : slip
D : diameter of bar
ε: bar strain

When significant plasticity distortion arises as a result of reinforcing bar yielding, the stress-strain characteristic of the reinforcing bars above the yield strain becomes important to the calculation of reinforcing bar pullout from footings. Therefore, the stress-strain curve of the longitudinal reinforcing bars in the analysis was modeled, including the strain hardening range. On the basis of previous studies[7][8], the stress-strain curve of the reinforcing bars was modeled such that it corresponds to the stress-strain curve obtained in tensile experiments on reinforcing bars.

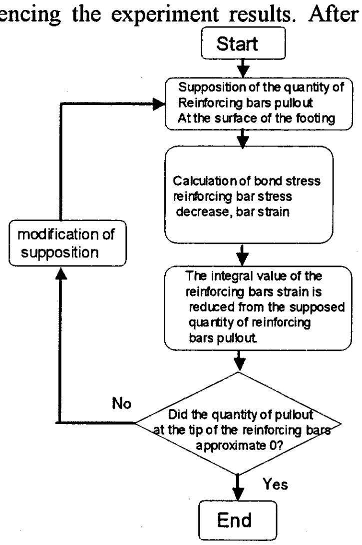

Figure 6 Analysis Flow Chart

An example of a reinforcing bar stress-strain curve used in the analysis is shown in Figure 7. The τ-s-ε relationship shown in Equation (3) was proposed from the results of ideal tensile experiments in which deterioration of the bond is ignored. However, specimens did undergo reversed cyclic loading. Therefore, if Equation (3) is applied directly, there is a possibility that the amount of reinforcing bar pullout from the footings will be underestimated. In this examination, the range within which the bond stress between reinforcing bars and concrete deteriorates is taken into consideration. This range is determined from a repeated calculation so as to ensure that the analytical value corresponds to the experiment result for specimen K1. Further, in the case of specimen K1, the amount of reinforcing bar pullout is measured directly with a displacement meter in a cutout in the footing. As for the examination result in consideration of a range of this bond deterioration, details are given in the next clause.

The analytical values corresponded closely to the experimental results by decreasing the bond stress of the section of 3 times of the reinforcing bars diameter from the surface of footing from the viewpoint of straight line to become 0 at the surface of footing. It has been reported that the center-to-center spacing of reinforcing bars has an influence on the amount of pullout from the footings. According to Murayama's research [9], the influence of reinforcing bar spacing can be almost ignored in the amount of reinforcing bar pullout from the footings as long as the spacing of re-bars is at least three times the reinforcing bar diameter. As for the specimens used in this research, the spacing of reinforcing bars is are greater than three times the reinforcing bar diameter in all cases. Therefore, in the examination of reinforcing bars after yielding, only the deterioration of bonding by reversed cyclic loading was taken into consideration.

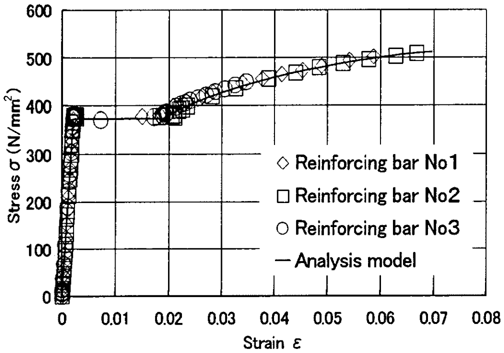

Figure 7 Strain-Stress Curve of Reinforcing Bar

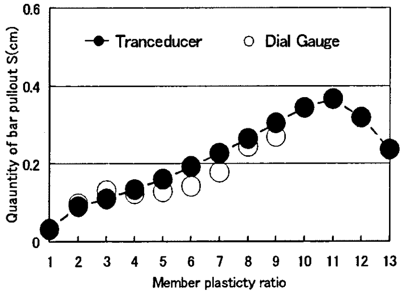

(a) Member Plasticity Ratio and Pullout of Re-bar

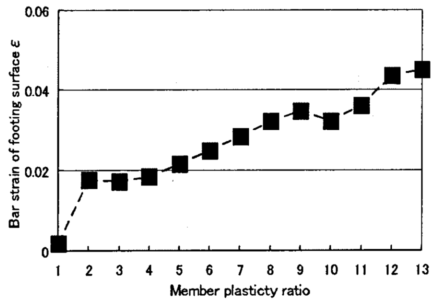

(b) Member Plasticity Ratio and Strain of Re-bar

Figure 8 Measurement Results for Specimen K1

4.2 Examination result toward the measurement value of the amount of pullout of the reinforcing bars of the K1 specimen

The member ductility ratio and the direct measurements of pullout, as well as the measured values of longitudinal reinforcing bar strain at the surface of the footings, are shown in Figure 8 up to the ultimate displacement. (The member ductility ratio is the value of lateral displacement in cyclic loading divided by the yield displacement (δy).)

Measurements with the dial gauge displacement meter could only be taken up to the load step 9δy. These measurements corresponded closely to the direct pullout measurements by displacement meter installed inside the footing cutout. This verifies that measurements taken with displacement meters installed inside cutouts in the footings are fully trustworthy.

The longitudinal reinforcing bar strain on the surface of the footing and the amount of reinforcing bar pullout increase in proportion to member ductility ratio, as shown in Figure 8. In particular, when the member ductility ratio is 8 or more, the strain of the longitudinal reinforcing bars at the surface of the footings exceeds 30,000μ.

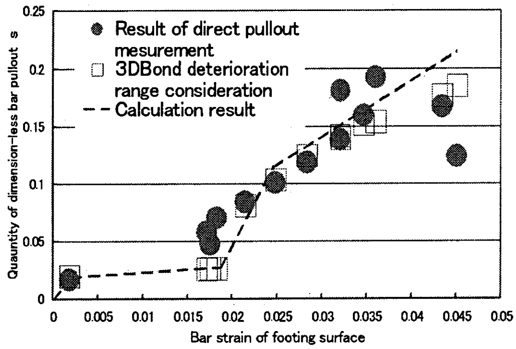

(b) Bond Deterioration Zone = 3D

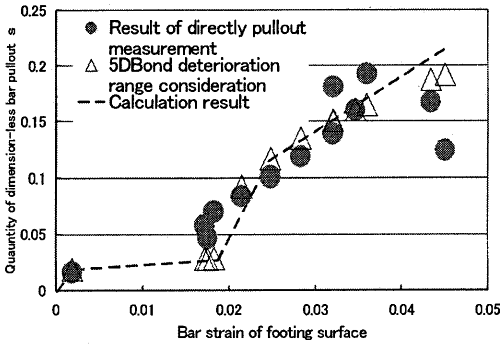

(b) Bond Deterioration Zone = 5D

Figure 9 Reinforcing Bar Strain at the Footing Surface and Comparison of Measured Pullout with Analytical Result

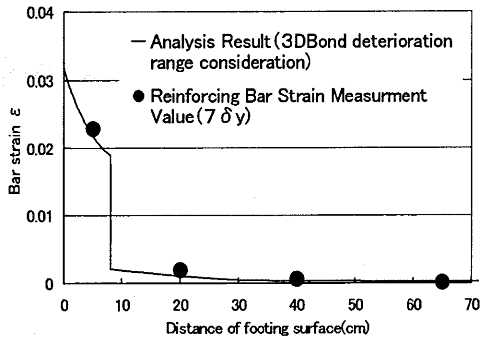

Figure 10 Relationship of Reinforcing Bar Strain Distribution Inside Footing and Comparison with Analytical Result (specimen a2)

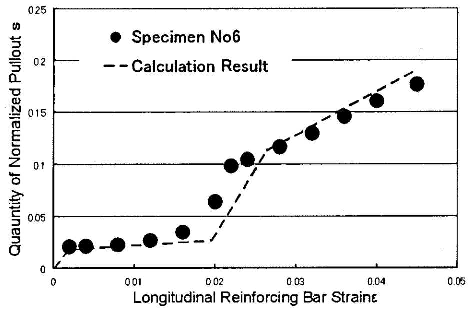

Figure 11 Relationship of Reinforcing bar Strain Distribution Inside Footing and Normalized Pullout (specimen No.6)

In Figure 9 (a) (b), the longitudinal reinforcing bar strain at the surface of the footings for each member ductility ratio is shown on the x-axis, while the measured value of reinforcing bar pullout from the footings is shown on the y-axis. The y-axis is made dimensionless using Equation (4).

$$s = S / D \cdot K_{fc} \qquad (4)$$

Where,
s : normalized value of reinforcing bar pullout
S : reinforcing bar pullout at footing surface
D: Diameter of bar, $K_{fc} = (f'_{ck}/20)^{2/3}$
f'_{ck}: concrete strength (N/mm^2)

Equation (4) is proposed in Shima's model of the relationship between reinforcing bar strain and slip[11]. Here, the pullout of the reinforcing bars (S) is made dimensionless by the reinforcing bar diameter (D).

The precision of the analytic result obtained with the relationship τ-s-ε that the bond deterioration range of the 3D section was taken into consideration from the surface of footing is comparatively better, and this explains the measurement result. However, measurement precision deteriorates when the strain of the longitudinal reinforcing bars at the surface of the footings exceeds 35,000μ. In the neighborhood of the ultimate displacement of a specimen under cyclic loading, the spalling of cover concrete and the buckling of re-bars affected the experimental results so much and they are not considered in analysis.Figure 9 (b) shows the analytical result when the bond deterioration range was moved into the 5D section from the surface of the footing in the same way as well.
This method is explained in reference [10]. It becomes somewhat larger by this method as compared with the measured value. From the thing above, it was decided to adopt the bond deterioration range of 3D in this

research.

4.3 Examination result of amount of reinforcing bar pullout in specimens except K1

Other specimens were examined using the same analysis method as used with specimen K1. In Table 1, specimens aside from K1 focus on measurements of the reinforcing bar strain at a position less than 50 mm from the surface of the footings. The reinforcing bar strain at the footing surface was estimated, and the reinforcing bars strain distribution that the measurement value of the reinforcing bars strain corresponded to the analytic result of the distortion distribution was calculated.

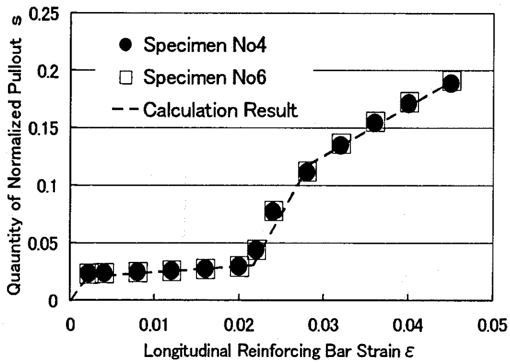

Figure 12 Relationship of Reinforcing bar Strain Distribution Inside Footing and Normalized Pullout (Specimen No.4 and No.5)

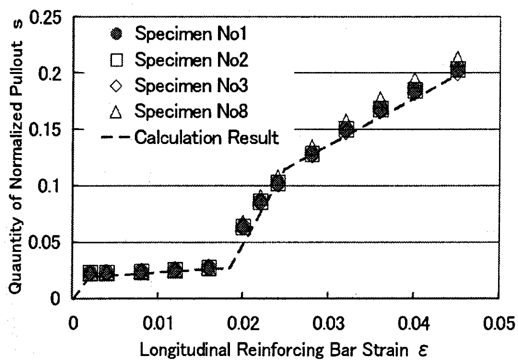

Figure 13 Relationship of Reinforcing bar Strain Distribution Inside Footing and Normalized Pullout (Specimen No.1, No.2, No.3, No.8)

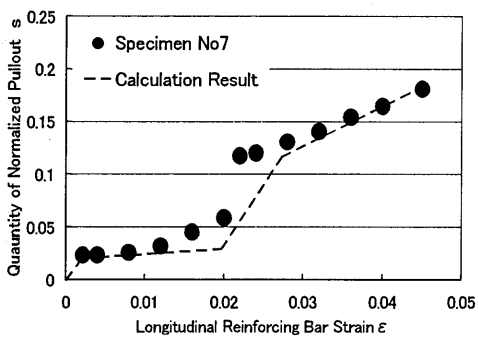

Figure 14 Relationship of Reinforcing bar Strain Distribution Inside Footing and Normalized Pullout (Specimen No.7)

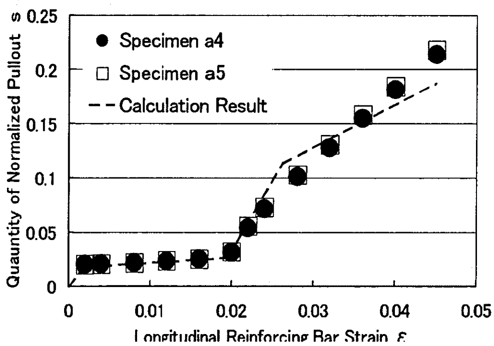

Figure 15 Relationship of Reinforcing bar Strain Distribution Inside Footing and Normalized Pullout (Specimen a4, a5)

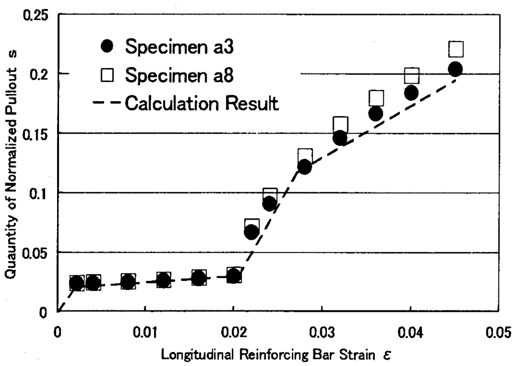

Figure 16 Relationship of Reinforcing bar Strain Distribution Inside Footing and Normalized Pullout (Specimen a3, a8)

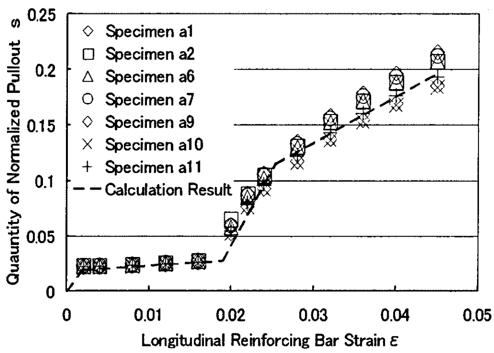

Figure 17 Relationship of Reinforcing bar Strain Distribution Inside Footing and Normalized Pullout (Specimen a1, a2, a6, a7, a9, a10, a11)

As an example, Figure 10 shows the result for 7δy, which becomes the biggest member ductility ratio that reinforcing bars strain is measured in specimen A2. The examination confirms that the measured reinforcing bar strain distribution can be calculated using this analysis.

This tells us that the amount of longitudinal reinforcing bar pullout from the footings can be determined as the integral of the reinforcing bar strain distribution calculated by analysis. When the value of the reinforcing bar distortion of the surface of footing was made to change, the measured amount of reinforcing bar pullout from the footings is shown in Figures 11 to 17 for each reinforcing bar classification used in the specimens.
The amount of reinforcing bar pullout from the footings is expressed in dimensionless form using Equation (4).

4.4 Formulation of longitudinal reinforcing bar strain at surface of footings and its relationship to dimensionless reinforcing bar pullout

It was decided to express the relationship between reinforcing bar strain at the footing surface and the dimensionless form of the reinforcing bar pullout using four straight lines corresponding to the strain level of the reinforcing bars. In the yield strain of reinforcing bars, the dimensionless reinforcing bar pullout was obtained with the equation proposed by Shima of the equation (5)[10][11]. The result obtained with Equation (5) corresponds closely to the experimental value and the analytical value.

In post-yield range of the reinforcing bars, it was decided that the dimensionless form of B of the reinforcing bars modified the model of the reinforcing bars strain -slip of monotonic loading by Sin. Equations (6) to (9) are the formulas proposed in this research. Equation (6) is the dimensionless reinforcing bar pullout in the range from the yield strain (εy) to strain hardening (εsh).

In Sin's model, there is no increase in the pullout in this range. However, the experimental results show pullout increasing, and the analytic result with being minute. Equation (6) takes this increase into consideration. In the post-strain-hardening range of reinforcing bar strain, Equations (7) and (8) approximate the situation with two straight lines. Finally, the strain (εa) at the point where the slope changes is given by Equation (9).
The values of dimensionless reinforcing bar pullout as computed by Equations (5) through (9) are shown by the dotted lines in Figure 9, and Figures 11 through 17. These calculated pullouts from the footings are comparatively precise.

In Figure 17, the difference between specimens A2 and A7 is the cyclic loading pattern. The other specimens are subject to the same conditions. The calculated reinforcing bar pullouts in these two cases are nearly the same, so no influence of cyclic load pattern is evident.

(a) Yield strain (εy) range

$$s = \varepsilon_y \ (2+3500\varepsilon_y\ ) \ {*}\alpha_y \qquad (5)$$

(b) Hardening strain (εsh) range

$$s = 0.5(\varepsilon_{sh} - \varepsilon_y) + s\ (\varepsilon_y\ ) \qquad (6)$$

(c) post-strain hardening of the reinforcing bar, the reinforcing bars strain (εa) of the point that the slope of the dimension-less slide change

$$s = 0.08\ (f_u - f_y)(\varepsilon_a\text{-}\varepsilon_{sh}) + s(\varepsilon_{sh}) \qquad (7)$$

(d) When reinforcing bars strain is larger than ε_a

$$s = 0.027(f_u - f_y)(\varepsilon_s\text{-}\varepsilon_a) + s(\varepsilon_a)$$

Where,
ε_y: yield strain of reinforcing bars
ε_{sh}: strain hardening limit of reinforcing bars

f_u: tensile strength of reinforcing bars (N/mm^2)
f_y: yield strength (N/mm^2) of reinforcing bars
ε_s: strain of reinforcing bars
α_y: influence of reinforcing bar spacing

$\alpha_y = 1+0.9e^{0.45(1-Cs/\phi)}$[12]

Cs: spacing of reinforcing bars
Φ: diameter of reinforcing bars
ε_a :post - strain hardening of the reinforcing bar, the reinforcing bars strain (ε_a) of the point that the slope of the dimension-less slide change

$$\varepsilon_a = \varepsilon_{sh} + \{(0.132 - s(\varepsilon_y)/2)/(0.13(f_u - f_y))\} \quad (9)$$

s (ε_y): dimensionless pullout in the yield strain range of reinforcing bars
s (ε_{sh}): dimensionless pullout at the point where the reinforcing bars are in hardening strain
s (ε_a): dimensionless pullout in ε_a has the strain of the reinforcing bars

5. Method of calculating reinforcing bar pullout from footings at ultimate displacement

5.1 Member ductility ratio and the examination of longitudinal reinforcing bar strain at the footing surface

In the formulas defining the relationships between longitudinal reinforcing bar strain at the footing surface and the dimensionless reinforcing bar pullout, the longitudinal reinforcing bar strain at the surface of the footings must be known in order to calculate the ultimate displacement. The strain is measured with wire strain gauges fitted to the reinforcing bars. However, in specimens subjected to cyclic loading, damage was concentrated on the base of the specimen, so it often proved impossible to take readings from the strain gauges during cyclic loading steps.

This problem was overcome by using specimen K1, for which the pullout was directly measured. The lead line of the wire-strain-gauge was fully lengthened, enabling the reinforcing bar strain to be measured up to the ultimate displacement.

Then, in specimens where the focus was reinforcing bar strain at points less than 50 mm below the surface of the footings, the reinforcing bar strain at the footing surface was assumed to correspond to the strain distribution of the measured reinforcing bars from the calculation by the analysis.

The relationship between member ductility ratio and reinforcing bar strain at the footing surface is shown in Figure 18.Figure 18 is fitted by Equation (10), which is shown by the straight line on the graph. This equation represents the relationship between member ductility ratio and reinforcing bar strain at the footing surface.

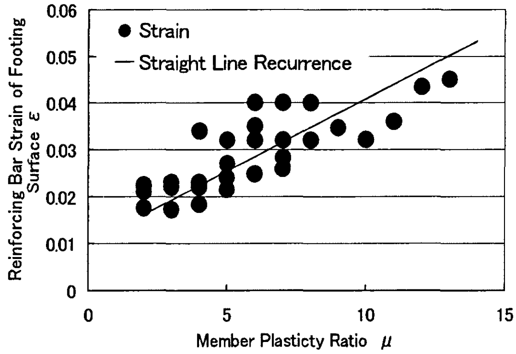

Figure 18 relationship between member ductility ratio and reinforcing bar strain at the footing surface

$$\varepsilon = 0.0031 \cdot \mu + 0.0099 \quad (10)$$

(correlation coefficient $\gamma = 0.819$)

Where, $2 \leqq \mu < 14$

$3.55 \leqq D/\phi \leqq 7.69$

(reinforcing bars arranged in a row)

ε: reinforcing bar strain at footing surface
μ: ductility ratio of the member at ultimate displacement
D: reinforcing bar spacing
Φ: reinforcing bar diameter

5.2 Calculation of reinforcing bar pullout from footings at ultimate displacement in actual structure

In the research described, the ductility ratio of the member at ultimate displacement is determined, and the reinforcing bar strain at the footing surface is computed from Equation (10). It then becomes possible to calculate the amount of pullout from the model of pullout of the reinforcing bars shown by the distortion of the reinforcing bars and Equation (5) Equation (9).

However, the reinforcing bar strain at the footing surface calculated from Equation (10) is based on the results of experiments using cyclic loading. Under seismic motion, however, it seems that damage occurs due to the elasto-plastic characteristics of the structure and the bonding between concrete and reinforcing bars may change.

In the member that the ductility ratio of the member becomes ultimate displacement around 10, the rotation of hinge of the plasticity is the most part with horizontal displacement. The proportion of the lateral displacement resulting from pullout of reinforcing bars at the ultimate displacement is thought to be relatively small in this situation.

As for errors in computing the reinforcing bar strain from Equation (10), it is considered that the influence this has on the ultimate displacement of the RC member is small. Based on this understanding, an examination of an actual structure is carried out below.

When it became ultimate displacement with ductility ratio of the member, an error of around 10,000μ is assumed in the reinforcing bar strain estimated from Equation (10). That is, a sensitivity analysis is carried out on the contribution of reinforcing bar pullout to ultimate lateral displacement when the reinforcing bar strain is made 10,000μ larger and smaller than the calculated value.

The railroad structure described in Reference [2] is examined, with analysis carried out on a column of the rigid frame bridge and the pier wall. Both in-plane and out-of-plane directions were considered in the case of the pier wall.

Equation (10) was applied to the out-of-plane direction of the pier wall, where the arrangement of longitudinal reinforcing bars is 2 rows. A general view of the examined structure is given in Figure 19. The properties of the structure are listed in Table 3.

The examination is carried out as follows. A model for reinforcing bar pullout from the footings was determined for each structure. The quantity of hoop reinforcement that results in the ultimate displacement at the ductility ratio of the decided member is calculated. The lateral displacement due to pullout of the reinforcing bars at the ultimate displacement is calculated. The ultimate displacement is calculated from the equation for member ductility given in Reference [5], given below as Equation (11). The method proposed in this paper is used for lateral displacement $\delta u1$ that originated in the rotation by pullout in ultimate displacement.

$$\delta_u = \mu \cdot \delta_y = \mu_0 \cdot \delta_{y0} + \delta_{ul} \qquad (11)$$

Where,
μ_0: ductility of pier member

μ_0=-1.9+6.6・(Su・a/Mu)+(13Pw-1.6)・Pw

Su: shear strength
a: shear span
Mu: ultimate flexural moment
Pw: shear reinforcement ratio
δ_{y0}: displacement of member at yield
δ_{u1}: ultimate displacement due to rotation by pullout of longitudinal reinforcing bars

$$\delta_{u1}= (S/d\text{-}x)\cdot la \qquad (12)$$

la: distance of the calculated lateral displacement position from surface of footings

(shear span or member length)

S: ultimate reinforcing bar pullout
d: effective depth
x: distance from the neutral axis to the compressive end

The lateral displacement originating in reinforcing bar pullout at the ultimate displacement can be calculated from Equation (12), multiplying the rotational angle of the pier body by the pullout of reinforcing bars from the footings and the shear span or member length.
The rotational angle can be calculated by dividing the amount of reinforcing bar pullout by the distance to the tension bar from the neutral axis of the section.

In specimen K1, the rotational angle was determined from the dial displacement gauge measurement and the measured pullout using Equation (12) and compared with the calculation. The measured value was larger by about 7%.

RC piers at ultimate displacement under cyclic loading tend to suffer column spalling of the cover concrete and damage to the strip. In determining the neutral axis at the ultimate displacement, this damage must be taken into account. In this examination, as a section of this damage condition, it was decided as a section which removed cover concrete to tension bar from tensile extreme from compressive extreme to compression bar. The neutral axis position was determined using the same method as used for maximum strength as shown in Section 3 (1), yield load/maximum load, and the rotation angle of the pier body was calculated. The calculated lateral load in the section that removed cover concrete is shown in Table 1. And, the comparison of the experiment value of lateral load of yield with lateral load that was calculated in the section which removed cover concrete is shown in Figure 20. The two values correspond comparatively well. The above demonstrates that the member condition of ultimate displacement is

Table 3 General View of Structures

Rigid frame structure		Pier	
type	RC beam-slab rigid frame type	type	RC-Pier Wall
track	slab track	type of foundation	spread foundation
spans	7 (Longitudinal Direct) 1 (Transverse Direct)	type of superstructure	PPC I section simple beam
column section	80cm×80cm	section of	150cm×400cm
height	8.05m (footing surface~slab top)	member height	7.0m (footing surface ~top of member)

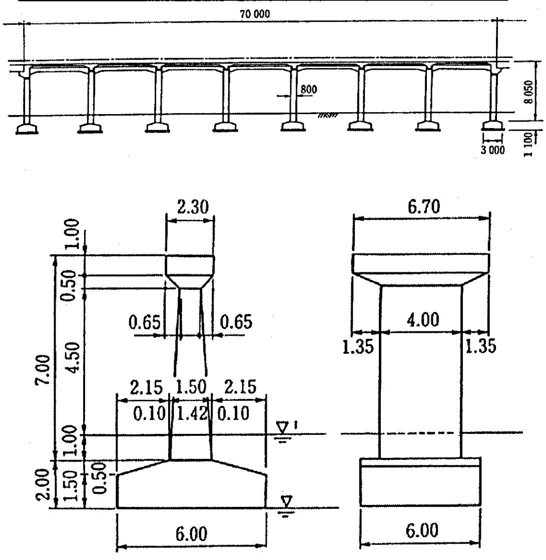

Figure 19 General View of Structures

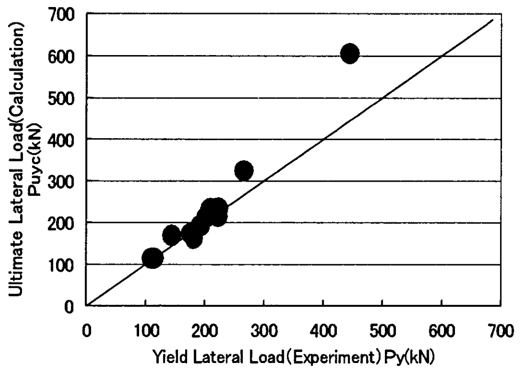

Figure 20 Comparison of Experiment Value of Lateral Yield Load and Lateral Load Calculated in the Section which Removed Cover Concrete

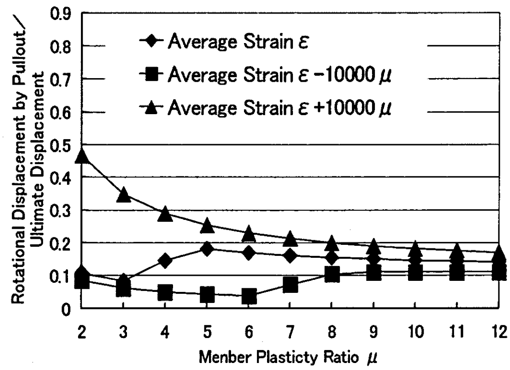

Figure 21 Proportion of Lateral Displacement due to Reinforcing Bar Pullout at Ultimate Displacement for Column of Rigid Frame Structure

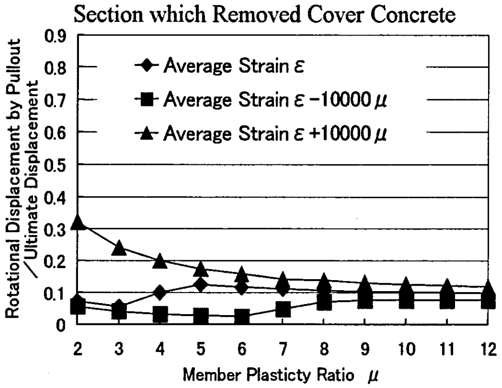

Figure 22 Proportion of Lateral Displacement due to Reinforcing Bar Pullout at Ultimate Displacement Rate of lateral displacement due to reinforcing bar pullout to ultimate displacement for Out-of-plane Direction of Pier Wall

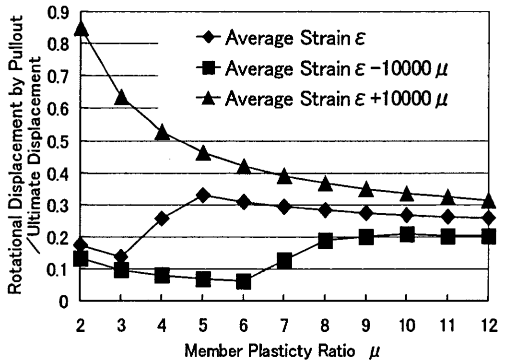

Figure 23 Proportion of Lateral Displacement due to Reinforcing Bar Pullout at Ultimate Displacement Rate of lateral displacement due to reinforcing bar pullout to ultimate displacement for In-plane Direction of Pier Wall

almost expressed suitably with the neutral position shaft that was calculated in the section which removed cover concrete.

The calculated amount of lateral displacement originating from reinforcing bar pullout at the ultimate displacement in the actual structure is shown in Figures 21 to 23. These figures show that when the ductility ratio of the member increases, the proportion of lateral displacement originating from pullout of the reinforcing bars falls. It is the case that the ductility ratio of the member becomes ultimate displacement with 10.

At the ultimate displacement, the proportion of lateral displacement originating from reinforcing bar pullout takes the following values:

About 11%-18 % for the column of the rigid frame bridge.
About 8%-12 % in the out-of-plane direction of the pier wall.
About 21%-33 % in the plane of the pier wall.

As for the reinforcing bar strain at the surface of footings, as calculated from Equation (10), a deviation of about 10,000μ caused it to change by only about 5% in each direction at a member ductility ratio of 10. Consequently, it can be concluded that the reinforcing bar strain as estimated from this equation does not have a major influence on the calculation of ultimate displacement.

6. Conclusion

The amount of reinforcing bar pullout from the footings is the basis for evaluating the seismic deformation reinforcing bar pullout. The research entailed carrying out cyclic loading tests on RC column specimens. The experiment results were analyzed for the -s- relationship in consideration of the bond deterioration range leading to the development of a calculation method that applies even to large deformation ranges (up to a ductility ratio of about 10). The application of the proposed equation to an actual structure was also examined. The following conclusions can be drawn from this work:

(1) The reinforcing bar pullout can be calculated accurately by Shima's bond-slip-strain model with an assumption that the bond deterioration zone is about 3D (D: diameter of re-bar).

(2) The amount of reinforcing bar pullout from the footings can be calculated by substituting reinforcing bar strains into the model of pullout given by Equations (5) to (9). Then, the reinforcing bar strain at the surface of the footings can be calculated from Equation (10).

(3) The neutral axis of the section at ultimate displacement can be calculated in the section where cover concrete was ignored.

(4) In the actual structure, the lateral displacement originating from reinforcing bar pullout at the ultimate displacement was calculated. When the ductility ratio of the member is higher, the proportion of lateral displacement originating from pullout decreases. It is the case that the plasticity rate of the member becomes ultimate displacement with 10, the rate of lateral displacement by pullout of the reinforcing bars became the following value: about 11%-18 % for the column of a rigid frame bridge; about 8%-12 % in the out-of-plane direction of the pier wall; and about 21%-33 % in the plane of the pier wall.

References

[1] Oota,M., "An Experimental Study on the Behavior of Reinforced Concrete Bridge Piers under Cyclic Loading", Proc.of JSCE, No.292, pp.65-74, 1979 (in Japanese)
[2] JSCE, "Standard Specification for Design and Construction of Concrete Structures [Seismic Design], 1sted", Tokyo, 1996 (in Japanese)
[3]Shima,H., Lie-Liung,C., and Okamura,H., "Bond-Slip-Strain Relationship of Deformed Bars Embedded in Massive Concrete", Proc. of JSCE, No.378, pp.165-174, 1987 (in Japanese)
[4] Sin,G., "Finit Element Analysis of Reinforced Concrete Member Subjected to In-Plane Force", Doctorate thesis at Tokyo University,1988.6
[5] Ishibashi,T., and Yoshino,S., "Study on Deformation Capacity of Reinforced Concrete Bridge Piers under Earthquake", Proc. of JSCE, No.390/V-8, pp.57-66, 1988 (in Japanese)
[6] JRTI, "Railway Structures Standard Specification for Design of Concrete Structures", 1992 (in Japanese)
[7] Shim,H., Lie-Liung,C., and Okamura,H., "Bond Characteristics In Post yield range Of Deformed Bars", Proc.of JSCE , No.378/V-6, pp.213-220, 1987 (in Japanese)
[8] Ben KATO, "Mechanical properties of steel under load cycles idealizing seismic action", Bulletin Dinformation, No131, CEB, IABSE-CEB Symposium, May 1979
[9] Murayama,Y., "Study on Characteristic s of Seismic Hysteresis Restoring Force of Reinforced Concrete Pier and Main Tower Member", Doctorate thesis for Kyushu University,1994.6 (in Japanese)
[10] Okamura,H., and Maekawa,K., "Nonlinear Analysis And Constitutive Models of Reinforced Concrete"
[11] Shima,H., Chou,L., and Okamura,H., "Micro and Macro Models for Bond in Reinforced Concrete", Journal of the Faculty of Engineering, The University of Tokyo(B), Vol.XXXIX, No.2, pp.133-194, 1987
[12] Shima,H., Sinohara,K., and Morioka,H., "Influence Of Reinforcing Bars Space Which Exerts It On The Quantity Of Pullout Of Reinforcing Bars Embedded In Footing", Proc. of JCI Symposium on Ductility and Arranged Reinforcing Bars, pp.109-114, 1990 (in Japanese)